Analytica Chimica Acta 1120 (2020) 36–42

Contents lists available at ScienceDirect

Analytica Chimica Acta

journal homepage: www.elsevier.com/locate/aca

A DNA triangular prism-based fluorescent aptasensor for ultrasensitive detection of prostate-specific antigen

Seyed Mohammad Taghdisi [a, b, 1], Noor Mohammad Danesh [c, 1], Morteza Alinezhad Nameghi [d], Mohammad Ramezani [d], Mona Alibolandi [d], Khalil Abnous [d, e, *]

[a] Targeted Drug Delivery Research Center, Pharmaceutical Technology Institute, Mashhad University of Medical Sciences, Mashhad, Iran
[b] Department of Pharmaceutical Biotechnology, School of Pharmacy, Mashhad University of Medical Sciences, Mashhad, Iran
[c] Research Institute of Sciences and New Technology, Mashhad, Iran
[d] Pharmaceutical Research Center, Pharmaceutical Technology Institute, Mashhad University of Medical Sciences, Mashhad, Iran
[e] Department of Medicinal Chemistry, School of Pharmacy, Mashhad University of Medical Sciences, Mashhad, Iran

HIGHLIGHTS

- A fluorescent aptasensor was described for detection of prostate-specific antigen (PSA).
- The biosensor was based on DNA triangular prism, PicoGreen, streptavidin magnetic beads and RecJf exonuclease.
- The aptasensor was ultrasensitive for detection of PSA because of using the DNA origami.
- The detection limit of sensing method was 30 pg/mL for PSA.
- Applying the designed aptasensor, PSA was successfully detected in human serum samples.

GRAPHICAL ABSTRACT

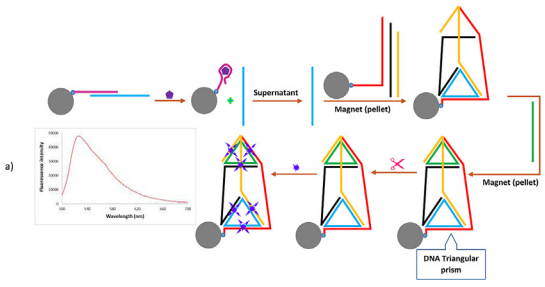

ARTICLE INFO

Article history:
Received 31 January 2020
Received in revised form
23 April 2020
Accepted 27 April 2020
Available online 30 April 2020

Keywords:
DNA triangular prism
Fluorescent aptasensor
Prostate-specific antigen
RecJf
Serum sample

ABSTRACT

In this study, a fluorescent aptasensor is described for ultrasensitive detection of prostate-specific antigen (PSA) using DNA triangular prism as a platform for attachment of fluorophore (PicoGreen, PG), streptavidin magnetic beads (SMBs) and RecJf exonuclease as enhancers of fluorescence difference between presence and absence of target. Presence of PSA leads to the formation of the DNA origami. So, a strong fluorescence is observed following the addition of PG. while, the DNA triangular prism cannot be formed in the lack of target. Thus, a very weak fluorescence can be measured after addition of PG. The proposed biosensor indicated high selectivity, a broad linear range from 200 pg/mL to 300 ng/mL and a very low detection limit of 30 pg/mL for PSA. Applying the designed aptasensor, PSA was successfully detected in human serum samples. This work provides a new way for detection of biomarkers in clinical samples.

1. Introduction

Prostate cancer is one of the most prevalent cancers among men and one of the leading causes of cancer death in men around the

* Corresponding author. Pharmaceutical Research Center, Pharmaceutical Technology Institute, Mashhad University of Medical Sciences, Mashhad, Iran.
E-mail address: abnouskh@mums.ac.ir (K. Abnous).
[1] These authors contributed equally to the work.

https://doi.org/10.1016/j.aca.2020.04.071
0003-2670/

world [1,2]. Prostate-specific antigen (PSA) as a glycoprotein is a reliable biomarker for diagnosis of prostate cancer and assessment of response to chemotherapy and prostate function [3,4]. The PSA concentration in serum of healthy people is below 4 ng/mL and higher concentration is considered as a possibility of appearance of prostate cancer or other prostate diseases [5,6]. In this way, precise determination of PSA is important for screening of prostate cancer and evaluation of its progression.

To date, different traditional techniques, such as chemiluminescent immunoassay [7], surface-enhanced Raman scattering (SERS) [8], radioimmunoassay [9], enzyme-linked immunosorbent assay (ELISA) [10] and electrochemical immunoassay [11] have been presented for PSA detection. These methods are generally based on the application of antibody as sensing element. So, they suffer from the antibodies affiliated drawbacks such as high cost, low stability, time-consuming preparation and difficult procedure of antibodies modification [12–14].

Aptamers are short single-stranded sequences obtained by an *in vitro* combinatorial approach called Systematic Evolution of Ligands by Exponential enrichment (SELEX) [6,15]. They can recognize a wide range of targets with high selectivity and affinity by forming unique three-dimensional shapes [16]. Aptamers have numerous features over antibodies, including high chemical and thermal stability, cost-effectiveness, high uniformity, easy labeling and flexible modification [17–19]. According to these characteristics, aptamers, also known as chemical antibodies, have been broadly utilized to fabricate biosensors for detection of different targets.

In recent years, fluorescent sensors have been extensively used for detection of different substances due to their relative simplicity regarding analysis and instrumentation, high sensitivity and low-cost [20–22].

In the current study, a fluorescent aptasensor was presented for detection of PSA using a DNA triangular prism as a DNA origami structure, streptavidin magnetic beads (SMBs), RecJf exonuclease and PicoGreen (PG) as fluorescent dye. The proposed fluorescent aptasensor was ultrasensitive for detection of PSA because it has been confirmed that the DNA origami-based aptasensors commonly show more sensitivity for their targets in comparison with other kinds of sensing platforms [23]. Furthermore, the uses of SMBs and RecJf resulted in more improvement of the aptasensor sensitivity because in the absence of PSA, the DNA triangular prism was not formed and the free single-stranded sequences could be easily removed from the sample using a magnet. Also, RecJf could digest single-stranded DNAs (ssDNAs) on the surface of SMBs in the absence of PSA. So, a great fluorescence emission difference could be observed following the addition of PG between samples with and without target. Besides, for target binding, PSA aptamer (Apt) had to leave its complementary strand (ssDNA1), leading to increase the selectivity of the aptasensor.

2. Materials and methods

2.1. Materials

PSA aptamer (Apt) [24,25] and other ssDNAs were purchased from Microsynth (Switzerland, Table S1). Immunoglobulin G (IgG), human serum albumin (HSA), and carcinoembryonic antigen (CEA) were ordered from Sigma-Aldrich (USA). Alpha-fetoprotein (AFP) was ordered from ProSpec (Germany). Prostate-specific antigen (PSA) was obtained from Lee BioSolutions (USA). Streptavidin magnetic beads (SMBs) and RecJf were purchased from New England Biolabs (UK). PicoGreen (PG, 200x) was obtained from Invitrogen (USA). Human PSA ELISA kit was purchased from MyBioSource (USA).

2.2. Preparations of aptamer (Apt)-modified SMBs and ssDNA3-modified SMBs

1.2 mg SMBs was incubated with 10 μL biotin-labeled Apt (36 μM). Then, 20 mM Tris-HCl (pH 7.4) was used to adjust the sample volume to 400 μL and the sample was placed at room temperature for 1 h 10 μL biotin-labeled ssDNA3 (26 μM) was transferred to 1.2 mg SMBs in 20 mM Tris-HCl (pH 7.4, final volume 400 μL) and incubated for 1 h. 2.5% agarose gel electrophoresis (stained with GelRed) was applied to evaluate the formation of the complexes.

2.3. Detection of PSA in phosphate buffer saline (PBS)

The process of PSA detection was as follows: 200 μL Apt-modified SMBs (0.9 μM Apt) was first added to 200 μL ssDNA1 (0.9 μM) for 1.5 h at room temperature, followed by 2.5% agarose gel electrophoresis analysis (Fig. S1). 50 μL of the above mixture (dsDNA-modified SMBs, 80 nM) was incubated with 50 μL PBS (5 mM, pH 7.4) containing various amounts of PSA (0–600 ng/mL) for 1 h at room temperature. A strong magnet (DynaMag™) was utilized to collect the supernatants. The supernatants were treated with 7 μL ssDNA2, 7 μL ssDNA3-modified SMBs and 7 μL ssDNA4 (the final concentration of each strand was 40 nM) for 2 h at room temperature, followed by removing supernatants using the magnet. 7 μL ssDNA5 (40 nM final concentration) was added to each sample and incubated for 2 h, followed by removal of supernatants using the magnet. 50 U/mL RecJf was added to each sample and incubated at 37 °C for 90 min. Finally, the supernatants were discarded by the help of magnet and 10 μL PG (15x) was transferred to each sample (final volume 100 μL). After incubation for 10 min at room temperature, fluorescence intensities (λ_{Ex} = 480 nm and λ_{Em} = 525 nm) were recorded using the Synergy H4 microplate reader (BioTeK, USA).

2.4. Interference study of the sensing approach

To evaluate the selectivity of the DNA origami-based aptasensor for PSA detection, the response of aptasensor towards a number of possible interferents such as HSA, IgG, CEA and AFP was measured. The concentration of each interferent was 300 ng/mL.

2.5. Determination of PSA in serum samples

To evaluate the practicality of the designed approach, the developed method was utilized to measure the concentration of PSA in spiked serum samples as mentioned before. It should be noted that a simple pre-treatment was performed and serum samples were diluted 7-fold with 5 mM PBS (pH 7.4).

3. Results and discussion

3.1. Principle of the method

By taking the advantage of DNA origami-based approaches, a DNA triangular prism-based fluorescent aptasensor was developed for ultrasensitive determination of PSA. The SMBs and RecJf were applied to improve the sensitivity of the aptasensor.

PG is a fluorochrome which specifically interacts with dsDNA. Following binding to dsDNA, PG shows a high fluorescence enhancement (>1000-fold), while the free fluorochrome has no significant fluorescence. Also, it is stable to photobleaching [26–28]. RecJf is a ssDNA specific exonuclease which digests the ssDNA from 5′ to 3′ direction [29,30].

As shown in Scheme 1, in the presence of PSA, the released ssDNA1 was used as a foundation for the formation of DNA

triangular prism following the addition of other ssDNAs (ssDNAs2-5). Treatment with RecJf did not have any influence on the construction of DNA origami because no free 5′-terminus of ssDNA was available in the sample. So, strong fluorescence emission was recorded following the treatment with PG.

In the absence of PSA, no DNA origami was formed because of lack of presence of the released ssDNA1 in the sample. In the absence of other ssDNAs (ssDNAs2 and 4), ssDNA5 could not be hybridized with biotin-labeled ssDNA3 because of their very short complementary region (7 bp). So, the 5′-end of biotin-labeled ssDNA3 was digested by RecJf. Therefore, a very weak fluorescence emission was observed when the PG was added to the sample. Application of RecJf resulted in no presence of ssDNA3 on the SMBs and sample in the absence of target. Furthermore, application of SMBs led to easily discard ssDNAs2 and 4 from the sample when PSA was absent. Thus, this phenomenon led to increase the sensitivity of the aptasensor and the sensing method showed a very great fluorescence difference in the absence and presence of PSA.

3.2. Optimization of detection conditions

To provide a sensing platform with the maximum performance, various parameters, including concentrations of SMBs, RecJf and PG were optimized.

As shown in Fig. 1a and b, the bands of free biotin-labeled Apt (36 μM) and biotin-labeled ssDNA3 (26 μM) were respectively disappeared when the concentration of SMBs was 1.2 mg. So, 1.2 mg SMBs was the sufficient concentration for loading of the mentioned ssDNAs.

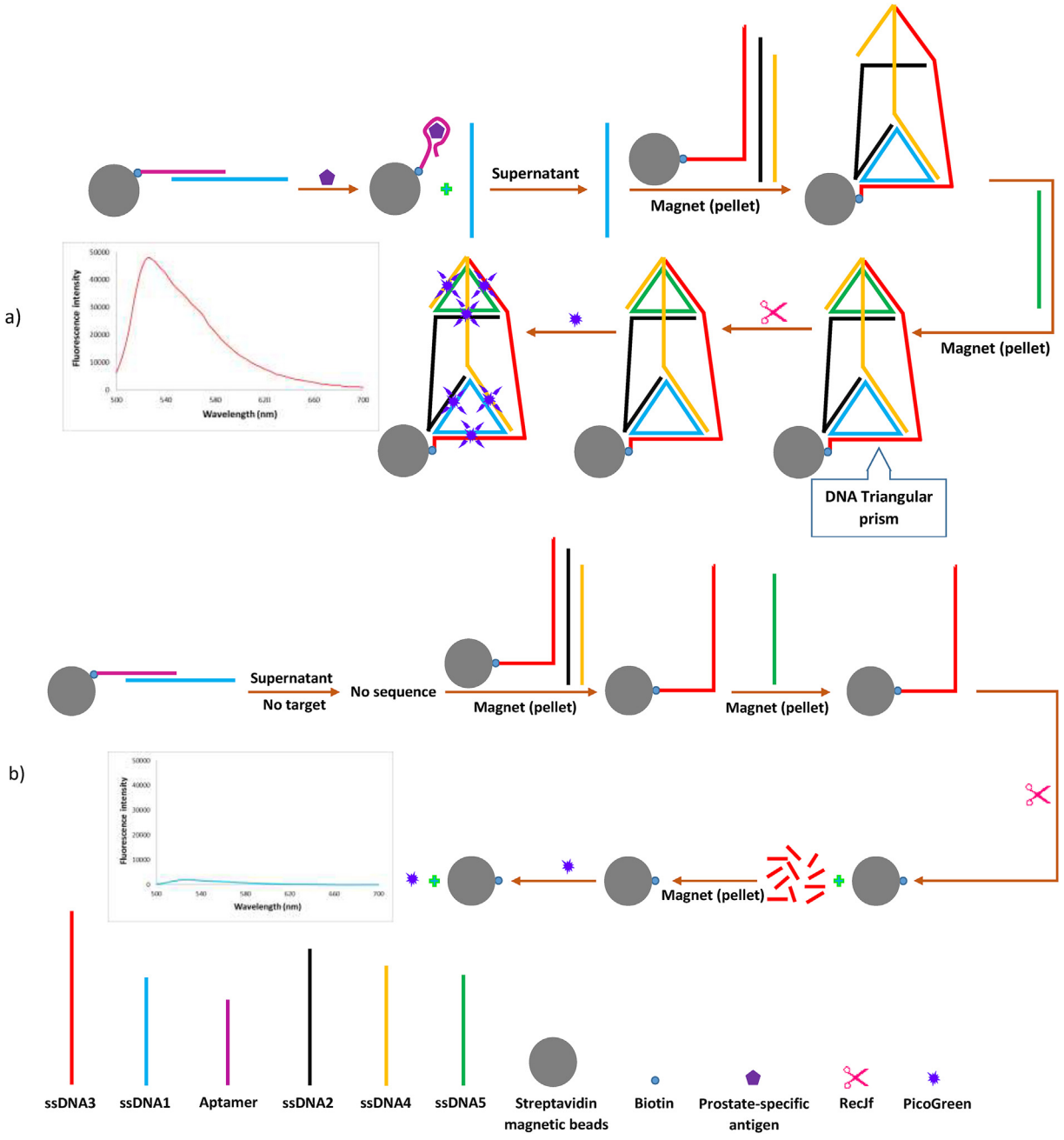

Scheme 1. Schematic illustration of the DNA triangular prism-based fluorescent aptasensor in the presence (a) and absence of PSA (b).

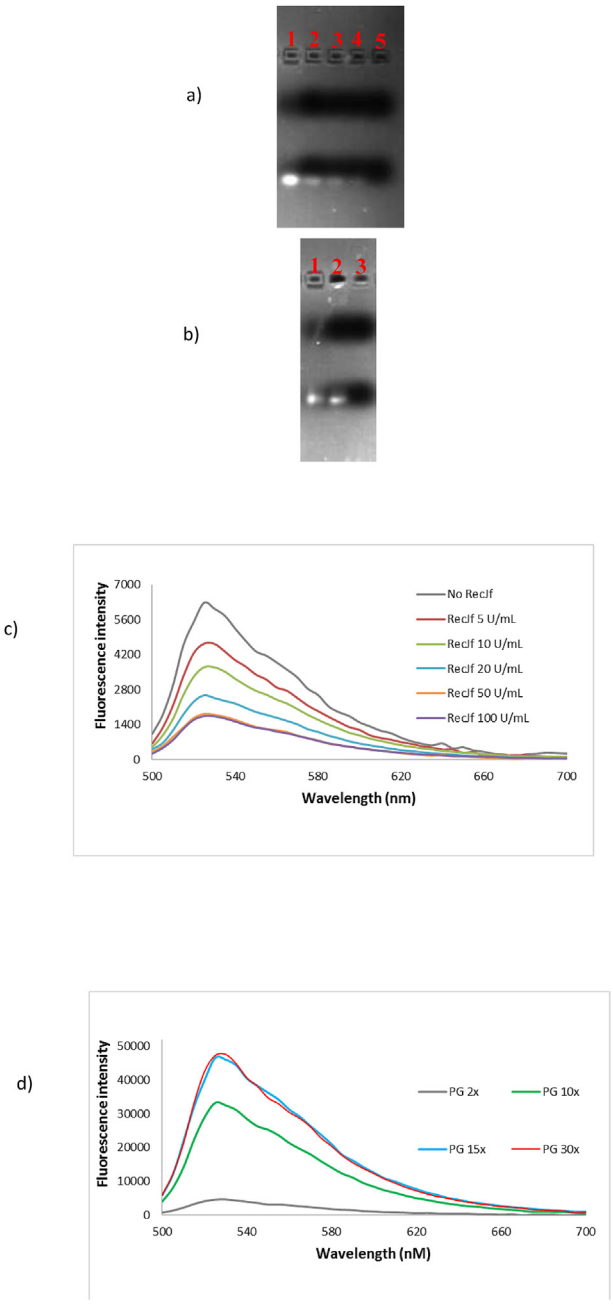

Fig. 1. Optimization of the aptasensor conditions. (a) Assessment of the capacity of SMBs for binding to biotin-labeled Apt. Lane 1: Apt (10 μL, 36 μM), lane 2: Apt + 0.3 mg SMBs, lane 3: Apt + 0.7 mg SMBs, lane 4: Apt + 1 mg SMBs, lane 5: Apt + 1.2 mg SMBs. (b) Assessment of the capacity of SMBs for binding to biotin-labeled ssDNA3. Lane 1: ssDNA3 (10 μL, 26 μM), lane 2: Apt + 0.7 mg SMBs, lane 3: Apt + 1.2 mg SMBs. (c) Fluorescence intensities under different concentrations of RecJf. (d) Fluorescence intensities under various amounts of PG.

The concentration of RecJf is another important parameter to affect the sensitivity of the aptasensor. As indicated in Fig. 1c, in the absence of target, the fluorescence response of aptasensor decreased with increasing the concentration of RecJf between 5 and 50 U/mL and then became constant. Therefore, 50 U/mL was obtained as the optimum concentration of RecJf.

In another experiment, the effect of the concentration of PG on the fluorescence signal was investigated in the presence of PSA (Fig. 1d). The result showed that the fluorescence response was maximum when the concentration of PG was 15x. Thus, the optimum PG concentration was 15x.

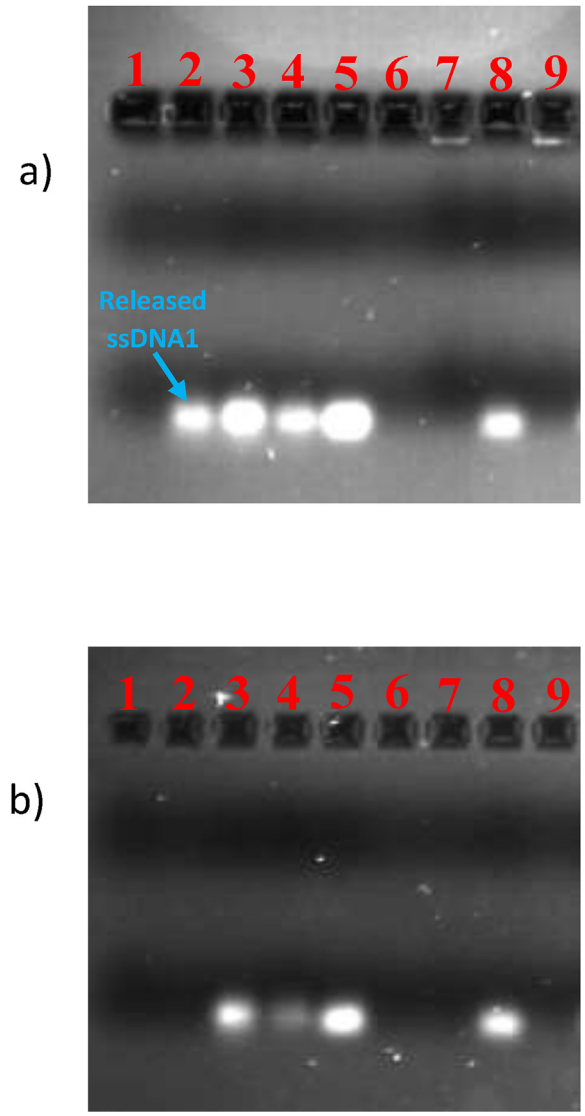

Fig. 2. Investigation of the fabrication and performance of the aptasensor using agarose gel electrophoresis (2.5%, stained with GelRed) in the presence (a) and absence of PSA (b). Lane 1: Apt/ssDNA1-modified SMBs, lane 2: Apt/ssDNA1-modified SMBs + PSA, lane 3: ssDNA1, lane 4: ssDNA2, lane 5: ssDNA4, lane 6: ssDNA3-modified SMBs, lane 7: released ssDNA1 + ssDNA2 + ssDNA3-modified SMBs + ssDNA4, lane 8: ssDNA5, lane 9: released ssDNA1 + ssDNA2 + ssDNA3-modified SMBs + ssDNA4 + ssDNA5 (DNA triangular prism).

3.3. Characterization of the aptasensor fabrication and operation

Agarose gel electrophoretic mobility shift assay (Fig. 2) and the fluorescence measurement (Fig. S2) were applied to assess the production and performance of the sensing approach.

As exhibited in Fig. 2a, the band of free ssDNA1 appeared (lane 2) following the addition of PSA to Apt/ssDNA1-modified SMBs, indicating the binding between PSA and Apt and release of ssDNA1 from the surface of SMBs. A single bright band was observed at the top of gel (lane 7) when other sequences (ssDNA2, ssDNA4 and ssDNA3-modified SMBs) were incubated with the released ssDNA1, showing complete interaction between these ssDNAs and their presences in the surface of SMBs. In the presence of ssDNA5, there

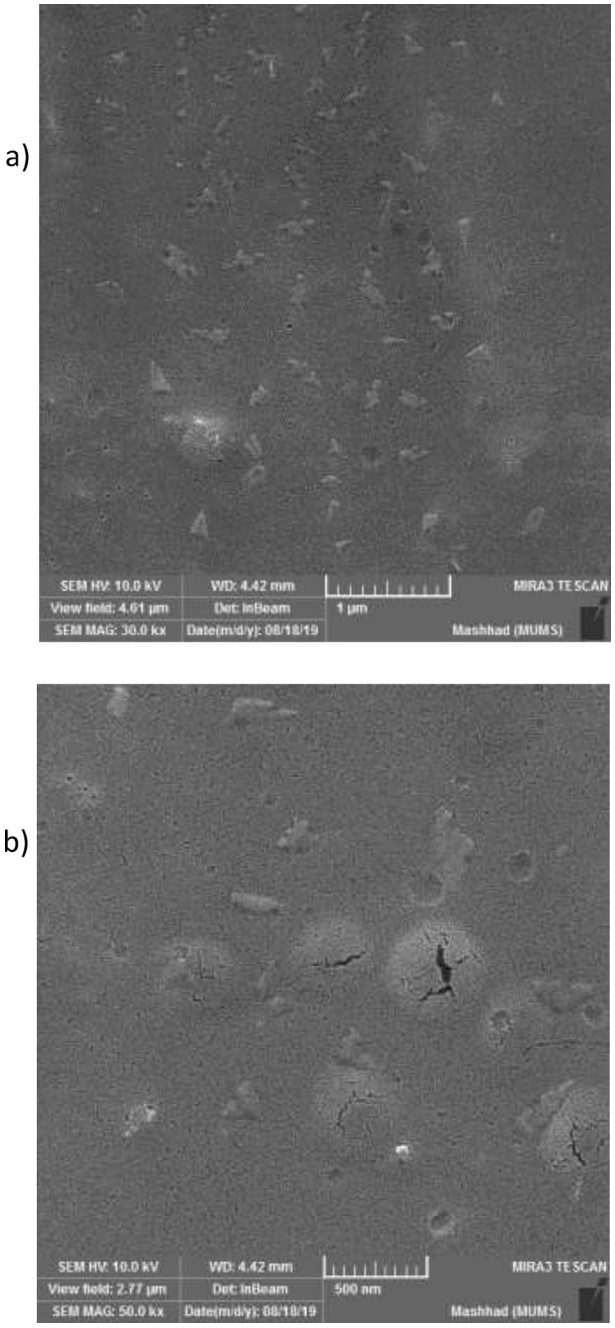

Fig. 3. SEM images of DNA triangular prism with different scale bars.

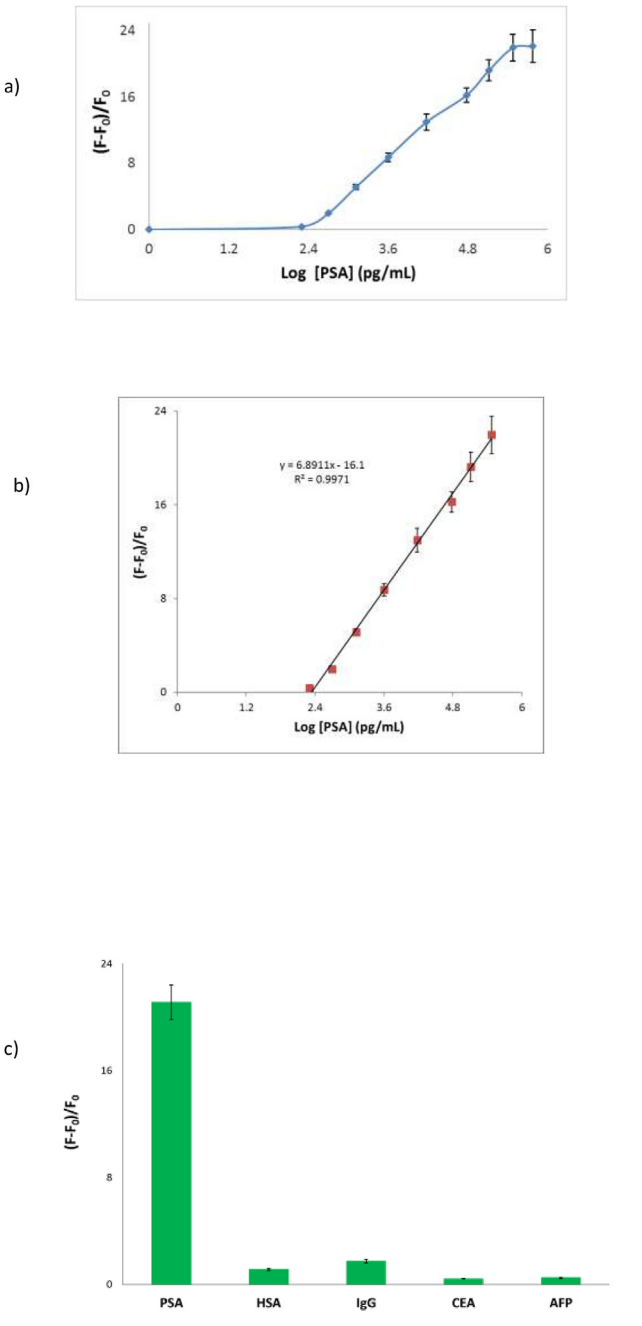

Fig. 4. (a) Relative fluorescence response of the aptasensor after adding different concentrations of PSA (0–600 ng/mL). (b) Linear relationship between the relative fluorescence response and logarithm of PSA concentration. F_0 and F are the fluorescence intensities (λ_{Em} = 525 nm) before and after addition of PSA, respectively. (c) Selectivity test. The relative fluorescence signal changes of the aptasensor in response to different proteins, including PSA, HSA, IgG, CEA and AFP. F_0 and F are the fluorescence intensities (λ_{Em} = 525 nm) before and after addition of each protein, respectively.

was a single brighter band at the same migration location (lane 9), confirming the self-assembly of the DNA triangular prism was successful. Also, the formation of this DNA origami was endorsed by the scanning electron microscopy (SEM, TESCAN MIRA3 microscope, Czech Republic) images (Fig. 3), too. In the absence of PSA (Fig. 2b), no free ssDNA band was observed (lane 2), showing the importance of the presence of target for release of ssDNA1. Also, following the addition of other sequences no band with low migration was observed (lanes 7 and 9), indicating the important role of ssDNA1 for the formation of the DNA triangular prism.

The result of fluorescence measurement showed that a strong fluorescence response could be detected from the aptasensor in the presence of PSA (Fig. S2), implying the successful formation of the DNA origami and the entrapment of PG in its double-stranded regions. While, in the absence of PSA, the sensing method displayed a very weak fluorescence signal because there was no DNA origami in the sample, confirming the significant role of PSA for the formation of DNA triangular prism. Also, the result exhibited that the application of RecJf could make more fluorescence different in the absence and presence of PSA, confirming its role for the improvement of aptasensor sensitivity.

Table 1
Comparison of the presented biosensor with other reported PSA sensing approaches.

Method	LOD	Linear range	Reference
Multicolor and photothermal dual-readout biosensor for visual detection of PSA	0.31 ng/mL	Not reported	[31]
An integrated magnetic microfluidic chip for immunodetection of the PSA using immunomagnetic beads	0.1 ng/mL	0.1–20 ng/mL	[32]
Gold nanoparticle triggered dual optoplasmonic-impedimetric sensing of PSA on interdigitated porous silicon platforms	1 ng/mL	0.1–500 ng/mL	[33]
Target-triggered signal-on ratiometric electrochemiluminescence sensing of PSA based on MOF/Au/G-quadruplex	0.058 ng/mL	0.5–500 ng/mL	[34]
Visual electrochemiluminescence ratiometry on bipolar electrode for bioanalysis	0.5 ng/mL	1–1000 ng/mL	[35]
Gold nano disks arrays for localized surface plasmon resonance based detection of PSA cancer marker	1.49 ng/mL	1.7–20.4 ng/mL	[36]
Label-free electrochemical aptasensing platform based on mesoporous silica thin film for the detection of PSA	0.28 ng/mL	1–300 ng/mL	[37]
Our fluorescent aptasensor	0.03 ng/mL	0.2–300 ng/mL	Current study

3.4. Analytical performance of the biosensor for PSA detection

The relative fluorescence response of the aptasensor induced by various concentrations of PSA has been presented in Fig. 4a. As shown in the figure, with increasing the amount of PSA, the relative fluorescence signal of the sensing method enhanced gradually. The linear range between the relative fluorescence signal and logarithm of PSA concentration was 200 pg/mL-300 ng/mL (Fig. 4b). The limit of detection (LOD) was measured to be 30 pg/mL in terms of the rule of signal-to-noise ratio of 3. The designed aptasensor showed satisfying performance for PSA determination with improved sensitivity and a wide linear range in comparison with other approaches for detection of PSA (Table 1) [31–37].

3.5. Selectivity of the DNA origami-based biosensing system

To validate the aptasensor selectivity, the sensing method was treated with different interfering proteins, including HSA, IgG, CEA and AFP. As indicated in Fig. 4c, the added interfering proteins exhibited very less impact on the relative signal intensities. However, upon addition of PSA an obvious signal change was detected, confirming high selectivity of the proposal analytical system for PSA.

3.6. Analysis of PSA in serum samples

To validate the effectiveness of the proposed aptasensor in real samples, PSA was spiked into human serum samples and the samples were analyzed using the aptasensor. As indicated in Table S2, the recoveries and relative standard deviations (RSDs) for the spiked PSA serum samples were 91.2–97% and 3.2–7.6%, respectively. The aptasensor showed acceptable recovery assay compared to commercial human PSA ELISA kit (Table S3). These results indicate that the DNA origami-based aptasensor has great potential for detecting PSA in real samples with high accuracy and reproducibility.

4. Conclusion

In this work, a novel fluorescent aptasensor was presented to determine very low concentration of PSA based on DNA triangular prism. Applications of the DNA origami, SMBs and RecJf resulted in remarkable fluorescence difference between presence and absence of target which showed excellent detection performance for PSA. The sensing platform has benefits, such as high sensitivity and selectivity which are attributed to its DNA origami structure and target-induced release of complementary strand, respectively. The linear range obtained from fluorescence was 200 pg/mL-300 ng/mL and LOD was 30 pg/mL. However, the fabrication of the aptasensor needs multiple steps which increases the time of PSA detection. Also, the aptasensor was used to determine PSA in human serum samples. The results exhibited good precision and accuracy of the approach. The designed sensing approach provides great opportunity for detection of PSA in biological samples and can be applied for detection of other targets by simply replacing the corresponding sequences.

Declaration of competing interest

The authors declare that they have no known competing financial interests or personal relationships that could have appeared to influence the work reported in this paper.

CRediT authorship contribution statement

Seyed Mohammad Taghdisi: Writing - original draft, Investigation, Data curation, Conceptualization. **Noor Mohammad Danesh:** Writing - original draft, Data curation, Formal analysis. **Morteza Alinezhad Nameghi:** Writing - review & editing. **Mohammad Ramezani:** Writing - review & editing, Methodology. **Mona Alibolandi:** Writing - review & editing, Methodology. **Khalil Abnous:** Conceptualization, Project administration, Funding acquisition, Writing - review & editing.

Acknowledgments

Financial support of this study was provided by Mashhad University of Medical Sciences.

Appendix A. Supplementary data

Supplementary data to this article can be found online at https://doi.org/10.1016/j.aca.2020.04.071.

References

[1] C. Pothipor, N. Wiriyakun, T. Putnin, A. Ngamaroonchote, J. Jakmunee, K. Ounnunkad, R. Laocharoensuk, N. Aroonyadet, Highly sensitive biosensor based on graphene–poly (3-aminobenzoic acid) modified electrodes and porous-hollowed-silver-gold nanoparticle labelling for prostate cancer detection, Sensor. Actuator. B Chem. 296 (2019) 126657.
[2] R. Gao, Z. Lv, Y. Mao, L. Yu, X. Bi, S. Xu, J. Cui, Y. Wu, SERS-based pump-free microfluidic chip for highly sensitive immunoassay of prostate-specific antigen biomarkers, ACS Sens. 4 (2019) 938–943.
[3] P. Karami, H. Khoshsafar, M. Johari-Ahar, F. Arduini, A. Afkhami, H. Bagheri, Colorimetric immunosensor for determination of prostate specific antigen using surface plasmon resonance band of colloidal triangular shape gold nanoparticles, Spectrochim. Acta Mol. Biomol. Spectrosc. (2019) 222.
[4] M. Li, P. Wang, F. Pei, H. Yu, Y. Dong, Y. Li, Q. Liu, P. Chen, A novel signal amplification system fabricated immunosensor based on Au nanoparticles and mesoporous trimetallic PdPtCu nanospheres for sensitive detection of prostate specific antigen, Sensor. Actuator. B Chem. 261 (2018) 22–30.
[5] Y. Zhao, W. Gao, X. Ge, S. Li, D. Du, H. Yang, CdTe@SiO2 signal reporters-based fluorescent immunosensor for quantitative detection of prostate specific antigen, Anal. Chim. Acta 1057 (2019) 44–50.
[6] A. Raouafi, A. Sánchez, N. Raouafi, R. Villalonga, Electrochemical aptamer-based bioplatform for ultrasensitive detection of prostate specific antigen, Sensor. Actuator. B Chem. (2019) 297.
[7] R. Liu, C. Wang, Q. Jiang, W. Zhang, Z. Yue, G. Liu, Magnetic-particle-based, ultrasensitive chemiluminescence enzyme immunoassay for free prostate-specific antigen, Anal. Chim. Acta 801 (2013) 91–96.
[8] T. Hao, X. Wu, L. Xu, L. Liu, W. Ma, H. Kuang, C. Xu, Ultrasensitive detection of

prostate-specific antigen and thrombin based on gold-upconversion nanoparticle assembled pyramids, Small 13 (2017).
[9] H.C.B. Graves, N. Wehner, T.A. Stamey, Ultrasensitive radioimmunoassay of prostate-specific antigen, Clin. Chem. 38 (1992) 735–742.
[10] A. Łupicka-Słowik, R. Grzywa, E. Leporowska, D. Procyk, J. Oleksyszyn, M. Sieńczyk, Development and evaluation of an immunoglobulin Y-based ELISA for measuring prostate specific antigen in human serum, Annals of Laboratory Medicine 39 (2019) 373–380.
[11] X. Zhao, J. Wang, H. Chen, H. Xu, L. Bai, W. Wang, H. Yang, D. Wei, B. Yuan, A multiple signal amplification based on PEI and rGO nanocomposite for simultaneous multiple electrochemical immunoassay, Sensor. Actuator. B Chem. (2019) 301.
[12] F. Ghorbani, H. Abbaszadeh, J.E.N. Dolatabadi, L. Aghebati-Maleki, M. Yousefi, Application of various optical and electrochemical aptasensors for detection of human prostate specific antigen: a review, Biosens. Bioelectron. (2019) 142.
[13] G. Liu, D.Q. Feng, Z. Li, Y. Feng, Target-activatable gold nanoparticle-based aptasensing for protein biomarkers using stimuli-responsive aggregation, Talanta 192 (2019) 112–117.
[14] Y. Sun, J. Fan, L. Cui, W. Ke, F. Zheng, Y. Zhao, Fluorometric nanoprobes for simultaneous aptamer-based detection of carcinoembryonic antigen and prostate specific antigen, Microchimica Acta 186 (2019).
[15] M. Chen, C. Ma, H. Zhao, Y. Yan, Exonuclease III-assisted fluorometric aptasensor for the carcinoembryonic antigen using graphene oxide and 2-aminopurine, Microchimica Acta (2019) 186.
[16] M. Hosseini Ghalehno, M. Mirzaei, M. Torkzadeh-Mahani, Electrochemical aptasensor for activated protein C using a gold nanoparticle – chitosan/graphene paste modified carbon paste electrode, Bioelectrochemistry 130 (2019).
[17] C. Chen, S. Feng, M. Zhou, C. Ji, L. Que, W. Wang, Development of a structure-switching aptamer-based nanosensor for salicylic acid detection, Biosens. Bioelectron. 140 (2019) 111342.
[18] Z. Bai, Y. Chen, F. Li, Y. Zhou, H. Yin, S. Ai, Electrochemical aptasensor for sulfadimethoxine detection based on the triggered cleavage activity of nuclease P1 by aptamer-target complex, Talanta 204 (2019) 409–414.
[19] K. Abnous, N.M. Danesh, M.A. Nameghi, M. Ramezani, M. Alibolandi, P. Lavaee, S.M. Taghdisi, An ultrasensitive electrochemical sensing method for detection of microcystin-LR based on infinity-shaped DNA structure using double aptamer and terminal deoxynucleotidyl transferase, Biosens. Bioelectron. 144 (2019).
[20] A. Ahmadi, N.M. Danesh, M. Ramezani, M. Alibolandi, P. Lavaee, A.S. Emrani, K. Abnous, S.M. Taghdisi, A rapid and simple ratiometric fluorescent sensor for patulin detection based on a stabilized DNA duplex probe containing less amount of aptamer-involved base pairs, Talanta 204 (2019) 641–646.
[21] M. Guo, Q. Hou, G.I.N. Waterhouse, J. Hou, S. Ai, X. Li, A simple aptamer-based fluorescent aflatoxin B1 sensor using humic acid as quencher, Talanta 205 (2019) 120131.
[22] M. Chen, C. Ma, Y. Yan, H. Zhao, A label-free fluorescence method based on terminal deoxynucleotidyl transferase and thioflavin T for detecting prostate-specific antigen, Anal. Bioanal. Chem. 411 (2019) 5779–5784.
[23] E. Sameiyan, E. Bagheri, M. Ramezani, M. Alibolandi, K. Abnous, S.M. Taghdisi, DNA origami-based aptasensors, Biosens. Bioelectron. 143 (2019).
[24] B. Wei, K. Mao, N. Liu, M. Zhang, Z. Yang, Graphene nanocomposites modified electrochemical aptamer sensor for rapid and highly sensitive detection of prostate specific antigen, Biosens. Bioelectron. 121 (2018) 41–46.
[25] Q. Zhou, Y. Lin, K. Zhang, M. Li, D. Tang, Reduced graphene oxide/BiFeO3 nanohybrids-based signal-on photoelectrochemical sensing system for prostate-specific antigen detection coupling with magnetic microfluidic device, Biosens. Bioelectron. 101 (2018) 146–152.
[26] J. Carvalho, R. Negrinho, S. Azinheiro, A. Garrido-Maestu, J. Barros-Velázquez, M. Prado, Novel approach for accurate minute DNA quantification on microvolumetric solutions, Microchem. J. 138 (2018) 540–549.
[27] C. Zhu, G. Zhang, Y. Huang, J. Yan, A. Chen, Aptamer based ultrasensitive determination of the β-adrenergic agonist ractopamine using PicoGreen as a fluorescent DNA probe, Microchimica Acta 184 (2017) 439–444.
[28] K. Abnous, N.M. Danesh, A. Sarreshtehdar Emrani, M. Ramezani, S.M. Taghdisi, A novel fluorescent aptasensor based on silica nanoparticles, PicoGreen and exonuclease III as a signal amplification method for ultrasensitive detection of myoglobin, Anal. Chim. Acta 917 (2016) 71–78.
[29] S. Yang, M. You, F. Zhang, Q. Wang, P. He, A sensitive electrochemical aptasensing platform based on exonuclease recycling amplification and host-guest recognition for detection of breast cancer biomarker HER2, Sensor. Actuator. B Chem. 258 (2018) 796–802.
[30] M. Chen, N. Gan, Y. Zhou, T. Li, Q. Xu, Y. Cao, Y. Chen, An electrochemical aptasensor for multiplex antibiotics detection based on metal ions doped nanoscale MOFs as signal tracers and Recj$_f$ exonuclease-assisted targets recycling amplification, Talanta 161 (2016) 867–874.
[31] Y. Wei, D. Wang, Y. Zhang, J. Sui, Z. Xu, Multicolor and photothermal dual-readout biosensor for visual detection of prostate specific antigen, Biosens. Bioelectron. 140 (2019).
[32] Z. Feng, S. Zhi, L. Guo, Y. Zhou, C. Lei, An integrated magnetic microfluidic chip for rapid immunodetection of the prostate specific antigen using immunomagnetic beads, Microchimica Acta 186 (2019).
[33] C. Rodriguez, V. Torres-Costa, O. Ahumada, V. Cebrián, C. Gómez-Abad, A. Díaz, M. Manso Silván, Gold nanoparticle triggered dual optoplasmonic-impedimetric sensing of prostate-specific antigen on interdigitated porous silicon platforms, Sensor. Actuator. B Chem. 267 (2018) 559–564.
[34] K. Shao, B. Wang, A. Nie, S. Ye, J. Ma, Z. Li, Z. Lv, H. Han, Target-triggered signal-on ratiometric electrochemiluminescence sensing of PSA based on MOF/Au/G-quadruplex, Biosens. Bioelectron. 118 (2018) 160–166.
[35] H.-J. Lu, W. Zhao, J.-J. Xu, H.-Y. Chen, Visual electrochemiluminescence ratiometry on bipolar electrode for bioanalysis, Biosens. Bioelectron. 102 (2018) 624–630.
[36] Y. Khan, A. Li, L. Chang, L. Li, L. Guo, Gold nano disks arrays for localized surface plasmon resonance based detection of PSA cancer marker, Sensor. Actuator. B Chem. 255 (2018) 1298–1307.
[37] W. Argoubi, A. Sánchez, C. Parrado, N. Raouafi, R. Villalonga, Label-free electrochemical aptasensing platform based on mesoporous silica thin film for the detection of prostate specific antigen, Sensor. Actuator. B Chem. 255 (2018) 309–315.